

Article

Production of Hemicellulose Sugars Combined with the Alkaline Extraction Lignin Increased the Hydro-Depolymerization of Cellulose from Corn Cob

Xiaorui Yang, Xiaotong Li, Liyan Zhu, Jinhua Liang and Jianliang Zhu *

College of Biotechnology and Pharmaceutical Engineering, Nanjing Tech University, 30 South Puzhu Road, Nanjing 211816, China; yangxiaorui@njtech.edu.cn (X.Y.); lixt0825@163.com (X.L.); 981314549@njtech.edu.cn (L.Z.); jhliang@njtech.edu.cn (J.L.)

* Correspondence: jlzhu@njtech.edu.cn

Abstract: Hydro-depolymerization is a novel method for converting agricultural waste into eco-friendly and promising products. Due to the complex structure and composition of corn cob (CC), a three-step process was developed, which involved pre-hydro-depolymerization of hemicellulose, alkaline extraction of lignin, and hydro-depolymerization of cellulose. The pre-hydro-depolymerization step was at first optimized to produce five-carbon and six-carbon sugars, achieving a maximum hemicellulose conversion rate of $78.48 \pm 3.92\%$, and reducing a sugar yield of $59.12 \pm 2.95\%$. Alkaline treatment achieved a maximum lignin extraction efficiency of $73.76 \pm 3.68\%$. After hemicellulose removal and delignification, the cellulose conversion rate increased to 36.63% and further increased to 76.97% after five cycles. Scanning electron microscopy (SEM) and Fourier transform infrared spectroscopy (FTIR) were performed to confirm physical and chemical changes in CC residues. The integrated process of hydro-depolymerization and alkaline treatment enables the complete exploitation of cellulose, hemicellulose, and lignin, and thus holds great potential for application in the agriculture industry.

Keywords: corn cob; hemicellulose sugars; lignin extraction; cellulose hydro-depolymerization; complete utilization



Citation: Yang, X.; Li, X.; Zhu, L.; Liang, J.; Zhu, J. Production of Hemicellulose Sugars Combined with the Alkaline Extraction Lignin Increased the Hydro-Depolymerization of Cellulose from Corn Cob. *Sustainability* **2023**, *15*, 9041. <https://doi.org/10.3390/su15119041>

Academic Editor: Marko Vinceković

Received: 3 May 2023

Revised: 29 May 2023

Accepted: 29 May 2023

Published: 2 June 2023



Copyright: © 2023 by the authors. Licensee MDPI, Basel, Switzerland. This article is an open access article distributed under the terms and conditions of the Creative Commons Attribution (CC BY) license (<https://creativecommons.org/licenses/by/4.0/>).

1. Introduction

Non-renewable chemical resources and fossil energy resources, such as oil, natural gas, and coal are limited and have negative impacts on the environment [1–5]. Thus, the search for renewable and environmentally friendly alternatives to fossil resources has become an urgent issue that needs to be addressed [6–8]. Lignocellulosic resources possess several advantages, including sustainability, cost-efficiency, reduced carbon footprint, abundant reserves, low added value, short regeneration time, and outstanding renewability [9–12]. As an alternative resource, lignocellulosic residues from forestry, herbs, and agricultural wastes, such as wheat straw, rice straw, rape stalk, corn stalk, and CC, have attracted extensive attention [13–17].

Every year, at least 1300 million tons of agricultural waste is produced, and the amount is likely to expand further in a world with a growing population to feed [18]. CC is a secondary agricultural residue that accounts for approximately 30% of maize agricultural wastes, with an estimated annual production of around 500 million metric tons globally [10,19]. Despite its potential as a biomass resource, CC has been underutilized, with direct incineration, animal feed production, or decomposition in the field being its main applications [20]. CC is mainly composed of three major biopolymers: cellulose (35.2~52.0%), hemicellulose (32.5~45.7%), and lignin (6.8~19.6%), as well as proteins, extractives, and ashes [21,22]. The polysaccharides content of CC makes it a potential source of available sugars, and its low ash content is advantageous for conversion processes [20]. In the

last decade, CC conversion has been investigated to obtain different products that can be more efficiently used as bio-adsorbents, thermal insulation materials, polymer composites, bioethanol and bioenergy chemicals, and other biomaterials for additional economic and ecological benefits [23–25]. However, lignin in CC's outer layer tightly intertwines and wraps around cellulose and hemicellulose, forming a dense, incorrigible, cross-linked three-dimensional (3D) structure known as lignocellulose. This structure significantly reduces the accessibility of catalysts to cellulose and hemicellulose, making subsequent conversion difficult [26,27]. In order to enhance accessibility and increase sugar yield by cellulose depolymerization, delignification is necessary, which can be achieved by either removing or separating the lignin and cellulose components using pretreatment methods [21]. Therefore, highly efficient pretreatment methods are essential before cellulose hydrolysis to improve the production of fermentable sugars [17].

Various chemical pretreatment methods have been developed for biomass, including acid leaching, dilute alkaline extraction, microwave pretreatment, ionic liquid pretreatment, ammonia fiber expansion, and organosolv extraction [28–30]. However, previous studies have suggested that certain pretreatments, such as microwave pretreatment, ionic liquid pretreatment, and ammonia fiber expansion, can be costly [10]. Additionally, the use of acidic media in a pretreatment can negatively affect the quality and energy yield of the biomass, as well as lead to the production of acidic wastewater, making acid leaching an unfavorable option [31,32]. Organosolv pretreatment can efficiently separate lignin and cellulose, but its harsh reaction conditions make it unsuitable for large-scale processes [33]. In contrast, alkaline pretreatment is an older and more gentle method that utilizes alkaline solutions such as sodium hydroxide (NaOH), calcium hydroxide (Ca(OH)₂), sodium carbonate (Na₂CO₃), and aqueous ammonia (NH₃·H₂O) [34]. Alkaline pretreatment causes the swelling and expansion of lignocellulose, affects lignin-carbohydrate ester bonds and hemicellulose acetyl groups in a series of reactions, and can effectively extract lignin and even silica, thereby making the lignocellulose surface more accessible for the reaction and ultimately improving catalytic accessibility to cellulose [34–36]. NaOH is the most commonly used alkali for pretreatment, and it shows promising results in extracting lignin for the production of fermentable sugars [37]. In addition, lignin extraction is beneficial for targeting the polysaccharide content of lignocellulose for depolymerization and conversion at high yields as well as integrating lignin recovery and utilization into lignocellulose biorefining processes [38].

It is noteworthy that when extracting lignin from holocellulose (which includes cellulose and hemicellulose), the process may degrade hemicellulose and reduce yields of sugars in subsequent conversion. Thus, it is essential to depolymerize hemicellulose before optimizing the pretreatment process for lignin extraction in order to make the most use of the holocellulose and efficiently remove lignin [17,39]. Catalytic hydrogenation can also be employed to degrade hemicellulose into xylose and arabinose, which can then be further converted into alcohols and sugar alcohols, thereby maximizing the utilization of lignocellulose.

A new integrated strategy to fully valorize all carbohydrates from CC and enhance its degree of depolymerization to yield large volumes of sugars is developed in this paper. The approach includes a three-step treatment process, which includes pre-hydro-depolymerization, alkali treatment, and final hydro-depolymerization. Pre-hydro-depolymerization was previously investigated to obtain hemicellulose sugars from CC; following which, alkali treatment was performed to dissolve the lignin that was acquired from the pre-depolymerized CC residues, thereby allowing the separation of cellulose. To achieve simultaneous sugar and lignin production while ensuring cellulose conversion, an optimal hydro-depolymerization condition was maintained. To understand the physical and chemical changes that occurred during the hydro-depolymerization and alkaline treatment of CC, a combination of scanning electron microscopy (SEM), Fourier transform infrared spectroscopy (FTIR), and specific surface area and porosity analyzer was employed. These techniques were used to analyze the resulting properties of the residues.

2. Materials and Methods

2.1. Materials and Reagents

The raw CC, rice straw, wheat straw, corn straw, and rape straw used in this study were all obtained from Puyang, Henan Province. They were then crushed using a pulverizer (JP-300B, Wenling Linda Machinery Co., Ltd., Wenling, China) to obtain particles of various sizes and sealed in for subsequent use. The CuO catalyst was obtained following the procedure presented in our previous study [40]. HCl (36.5 wt.%), NaOH, sulfuric acid (H₂SO₄), acetic acid, and ethanol were obtained from Sinopharm Chemical Reagent Co., Ltd., and were all of the analytical grades. Deionized water was purchased from Wahaha Group Co., Ltd., Hangzhou, China. Hydrogen (H₂) was obtained from Nanjing Special Gas Factory Co., Ltd., Nanjing, China, and the purity was 99.99%.

2.2. Hydro-Depolymerization of Agricultural Wastes

Raw materials (wheat straw, rice straw, corn straw, rape straw, and CC) with a particle size of 0.45–0.90 mm were subjected to a 2 h reaction in a high-pressure reactor (0.25 L, Weihai Chemical Machinery, Weihai, China) under the following conditions: reaction temperature, 140 °C; hydrogen pressure, 1.5 MPa; stirring speed, 500 r/min; material-to-water solid-to-liquid ratio, 1:10; and catalyst-to-material solid-to-solid ratio, 3:10. The resulting hydrolysates were filtered using a Brinell funnel with a diameter of 15 mm, and the supernatant fractions were collected for reducing sugar analysis using an ultraviolet-visible spectrophotometer (752S, Shanghai Shunyu Hengping Scientific Instrument Co., Ltd., Shanghai, China). Two reaction trials were performed twice under each condition.

2.3. Pre-Hydro-Depolymerization of Hemicellulose in CC

CCs with different particle sizes, CuO catalyst, and deionized water were evenly mixed and put into a reactor (0.25 L, Weihai Chemical Machinery, Weihai, China), sealed, and tightened, and the reaction was performed as reported previously [40]. The single-factor method included the following parameters: temperature range, 120 °C to 170 °C; particle size, 0.15 mm to 0.90 mm sieved by standard sieves (aperture of 0.15–0.90 mm, Nanjing Wire Mesh Factory, Nanjing, China); stirring speed, 200 r/min to 700 r/min; catalyst-to-CC (CAC) solid-to-solid ratio, 1:10 to 6:10; CC-to-water (CW) solid-to-liquid ratio, 1:7 to 1:10; reaction time, 1.0 h to 4.0 h; and H₂ pressure of 1.0 MPa to 3.5 MPa. The hydrolysates obtained after the reaction were filtered using a vacuum pump (Nanjingwin Instrument Equipment Co., Ltd., Nanjing, China), and the supernatant fractions were collected for sugar analysis by high-performance liquid chromatography (HPLC). The filters were washed with tap water, and the catalyst solutions were recovered. The samples were then dried at 60 °C, weighed, and subjected to analytical characterization. Each condition was repeated twice.

2.4. Alkali Pretreatment of Pre-Hydro-Depolymerized CC Residues (PHR)

The PHR and NaOH solutions were mixed in various proportions and evenly put into a reactor (0.25 L, Weihai Chemical Machinery, Weihai, China). The reaction conditions were as follows: the NaOH concentration ranged from 3% to 7% at a temperature of 80 °C to 120 °C; the PHR-to-water solid-to-liquid ratio ranged from 1:8 to 1:10; the time ranged from 1.0 to 5.0 h; and the catalyst-to-PHR solid-to-solid ratio ranged from 1:10 to 5:10. Following the completion of the reaction, acetic acid was used to neutralize the alkaline solution until the pH was nearly 5.5. Then, a rotary evaporator (ER52-AA, Shanghai Yarong Biochemical Instrument Factory, Shanghai, China) was employed to concentrate the liquid to 30 mL. Anhydrous ethanol was added to the concentrated solutions, vigorously stirred, filtered, and dried after precipitation and washing. The ethanol filtrate was further concentrated to 30 mL, the pH was adjusted to about 2.0 using 6.0 mol/L HCl, and acid-insoluble lignin was precipitated. The crude lignin was obtained by low-temperature drying after centrifugation by a centrifuge (TGL-10B, Shanghai Anting Scientific Instrument Factory, Shanghai, China) and stored in a dryer for further identification. All experiments were repeated twice.

2.5. Hydro-Depolymerization of Pre-Hydro-Depolymerized and Delignified CC Residues (PHRD)

The PHRD, catalysts, and deionized water were evenly mixed and placed into a reactor (0.25 L, Weihai Chemical Machinery, Weihai, China) using a process similar to that described in 2.3. An orthogonal experiment using four factors and three levels (Statistical Product and Service Solutions, International Business Machines Corporation, The United States of America) of PHRD hydro-degradation was then performed based on the single-factor method of hemicellulose. The objective of this part was to explore the optimal combination of reaction conditions for the hydro-depolymerization process. The stirring speed was set at 500 r/min, the H₂ pressure at 1.5 MPa, and the factors and levels considered were temperature (140~160 °C), CC-to-water solid-to-liquid ratio (1:8~1:10), catalyst-to-CC solid-to-solid ratio (2:10~4:10), and reaction time (1~3 h). Following the orthogonal experiment, the resulting hydrolysates were treated according to the process described in Section 2.3 to obtain the final residues (PHRDC). The reaction was performed twice under each condition. The hydro-depolymerization of PHRD residues was performed five times under the optimum condition of cellulose hydro-depolymerization; the reaction conditions were as follows: PHRD residues of 20 g, temperature of 140 °C, hydrogen pressure of 1.5 MPa, stirring speed of 500 r/min, a solid-to-solid ratio of 3:10, solid-to-liquid ratio of 1:10, and reaction time of 2 h.

2.6. Analysis of Agricultural Wastes and Hydrolysates

The National Renewable Energy Laboratory method [41] was used to determine the components of wheat straw, rice straw, corn straw, rape straw, CC, and CC residues. Each experiment was performed twice.

The concentration of the sugar solution was determined by HPLC (LC-20AD, Shimadzu Corporation, Kyoto, Japan). A RID-20A differential refraction detector was equipped, and the Aminex Hpx-87H (300 mm × 7.8 mm, Bio-Rad, Hercules, CA, USA) chromatographic column was used. Under the column temperature of 50 °C, a deionized water flow rate of 0.6 mL/min, and the automatic injection volume of 10 µL, each sample was injected thrice in parallel. Before injection, the samples were filtered and passed through a 0.45 µm water filter. The corresponding peak areas of sugars were obtained using HPLC, and calibration curves were generated (refer to Supplementary Figures S1–S3). Examples of the corresponding HPLC chromatograms are illustrated in Figures S4–S8 of the supplemental information.

The CC conversion and recovery rates were calculated as shown in Equations (1) and (2) [40]; cellulose conversion and recovery rates, hemicellulose conversion and removal rates, and lignin removal and extraction rates were calculated as shown in Equations (3)–(6) [5,20,40]; the lignin extraction rate (LER) was calculated as shown in Equation (7) [20].

$$\text{CC conversion} = \frac{\text{Mass of CC /PHR/PHRD} - \text{Mass of PHR/PHRD/ PHRDC}}{\text{Mass of CC/PHR/ PHRD}} \times 100\% \quad (1)$$

$$\text{CC Recovery} = \frac{\text{Mass of PHR/PHRD}}{\text{Mass of CC/PHR}} \times 100\% \quad (2)$$

$$\text{Hemicellulose conversion} = \frac{(\text{Mass of arabinose} + \text{mass of xylose}) \times 0.88}{\text{Mass of hemicellulose in CC}} \times 100\% \quad (3)$$

$$\text{Cellulose conversion} = \frac{\text{Mass of glucose} \times 0.9}{\text{Mass of cellulose in CC/PHRD}} \times 100\% \quad (4)$$

$$\text{Removal} = \left(1 - \frac{\text{Mass of lignin/hemicellulose in PHR/PHRD}}{\text{Mass of lignin/hemicellulose in CC/PHR}}\right) \times 100\% \quad (5)$$

$$\text{Cellulose Recovery} = \frac{\text{Mass of cellulose in PHR/PHRD}}{\text{Mass of cellulose in CC/PHR}} \times 100\% \quad (6)$$

$$\text{Lignin extraction} = \frac{\text{Mass of lignin recovery in pretreated liquid}}{\text{Mass of lignin in RHR}} \times 100\% \quad (7)$$

Reducing sugar yield (RSY) was analyzed by the 3,5-dinitrosalicylic acid method [42], as shown in Equation (8).

$$\text{RSY} = \frac{\text{Mass of reducing sugar}}{\text{Mass of CC/PHRD}} \times 100\% \quad (8)$$

2.7. Characterization of CC and Residues

The specific surface areas and aperture sizes of raw CC, PHR, and PHRD residues were determined using the specific surface area and aperture size analyzer (JW-BK122 W, Beijing Jingwei Gaobo Instrument Co., Ltd., Beijing, China). Under the presence of He and N₂, the temperature was increased at a rate of 10 °C/min to 105 °C, and the samples were kept at that temperature for 2 h to remove other impurities. Meanwhile, the samples were vacuumed for 2 h until the pressure was below 0.008 kPa. After cooling to room temperature, liquid nitrogen (approximately −196 °C) was added to the cold liquid nitrogen well (1 L) for analyzing the specific surface and apertures based on the multilayer adsorption theory [40].

FTIR (ALPHA, Bruker Cot., Karlsruhe, Germany) was employed to analyze and identify CC and its residues both before and after the reaction. The samples were pressed using KBr, dried, and ground to powder with a mortar. After that, the powder was evenly placed into a platinum groove with a smooth polishing surface. The samples were then read at the wavelength ranging from 4000 cm^{−1} to 400 cm^{−1}.

The surface morphologies of raw CC and treated residues were observed by SEM (JSM-5900, Electronics Co., Ltd., Tokyo, Japan). The samples were fixed onto a needle-type sample holder with carbon-coated conductive tape and were coated with gold for approximately 20 min. Images of the sample were captured under 15 kV voltage and enlarged by 2500×, as reported in our previous study [40].

3. Results and Discussion

3.1. Selection of Raw Materials

As presented in Table 1, different crop straws contain varying components. For instance, wheat straw, rice straw, corn stalk, rape stalk, and CC have different compositions.

Table 1. The main component and hydro-depolymerization results of the five ingredients.

Materials	Hemicellulose (%)	Cellulose (%)	Lignin (%)	CC Conversion (%)	Cellulose Recovery (%)	Lignin Removal (%)	Hemicellulose Removal (%)	RSY (%)
Rice straw	21.50 ± 1.00	39.86 ± 0.89	25.40 ± 1.17	44.87 ± 0.73	71.12	17.37	78.05	19.47 ± 0.21
Wheat straw	28.64 ± 0.93	35.13 ± 0.65	22.50 ± 1.02	46.55 ± 0.95	70.19	19.66	75.97	27.58 ± 0.18
Corn stalk	30.65 ± 0.42	36.43 ± 0.72	19.42 ± 0.90	44.32 ± 1.43	69.31	18.94	77.36	19.20 ± 0.62
Corn cob	32.50 ± 1.22	36.92 ± 0.74	18.22 ± 0.81	48.86 ± 0.93	68.54	20.38	80.29	32.42 ± 0.45
Rape stalk	23.13 ± 1.05	47.89 ± 0.99	19.07 ± 0.85	45.73 ± 1.26	72.98	18.87	77.32	20.77 ± 0.36

The amounts of lignin, cellulose, and hemicellulose in these crops significantly differ, which is likely due to variations in sampling, climatic, and cultivation conditions [23]. Among these raw materials, CC had a hemicellulose content of 32.50% and a cellulose content of 36.92%, which is similar to previous findings in the literature [43,44]. Under the same conditions, the RSY order of these crops was CC > wheat straw > rape stalk > rice straw > corn stalk. This finding further confirms that a higher hemicellulose content

results in a greater yield of reducing sugars. Therefore, CC was selected as the experimental material for studying its degradation process conditions in this research.

3.2. Pre-Hydro-Depolymerization of Hemicellulose in CC

To improve the comprehensive and efficient utilization of hemicellulose, it is recommended to fully utilize it prior to or during pretreatment to convert it into sugars, which are a valuable source of chemicals [15]. In this research, pre-hydro-depolymerization of CC was performed to degrade hemicellulose, and the effects of various conditions on the pre-hydro-depolymerization were investigated, as shown in Figures 1–7.

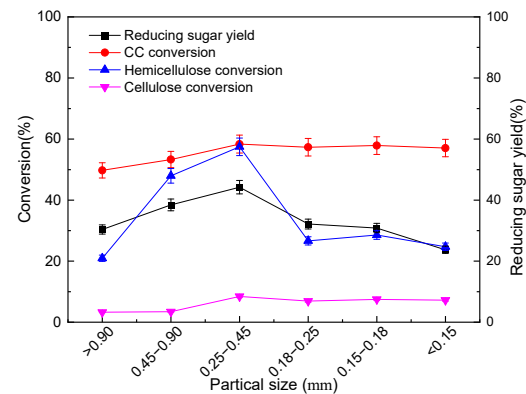


Figure 1. Effects of particle size on the pre-hydro-depolymerization of corn cob.

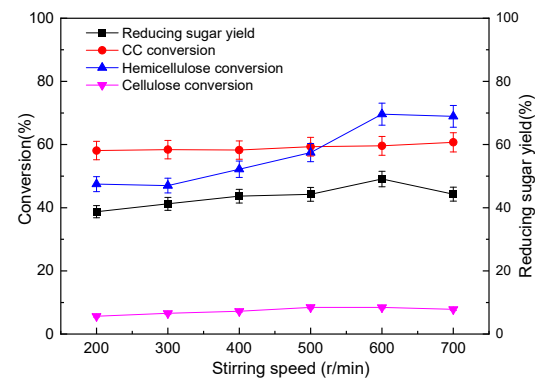


Figure 2. Effects of stirring speed on the pre-hydro-depolymerization of corn cob (CC particle size of 0.25–0.45 mm, temperature of 150 °C, time of 2 h, H₂ pressure of 1.5 MPa, CAC solid-to-liquid ratio of 1:10, CW solid-to-solid ratio of 3:10).

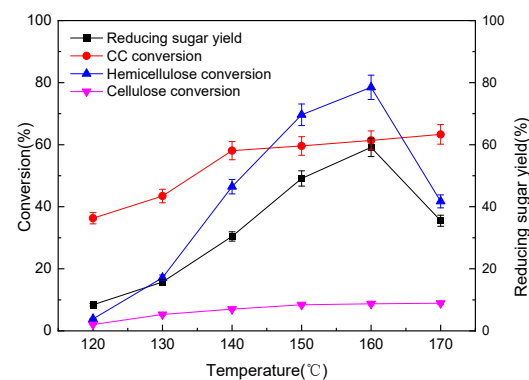


Figure 3. Effects of temperature on the pre-hydro-depolymerization of corn cob (CC particle size of 0.25–0.45 mm, stirring speed of 600 r/min, time of 2 h, H₂ pressure of 1.5 MPa, CAC solid-to-liquid ratio of 1:10, CW solid-to-solid ratio of 3:10).

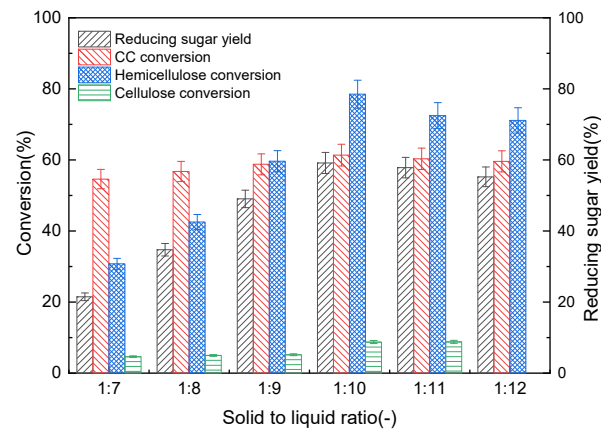


Figure 4. Effects of CAC solid-to-liquid ratio on the pre-hydro-depolymerization of corn cob (CC particle size at 0.25–0.45 mm, temperature at 160 °C, stirring speed at 600 r/min, time at 2 h, H₂ pressure at 1.5 MPa, CW solid-to-solid ratio at 3:10).

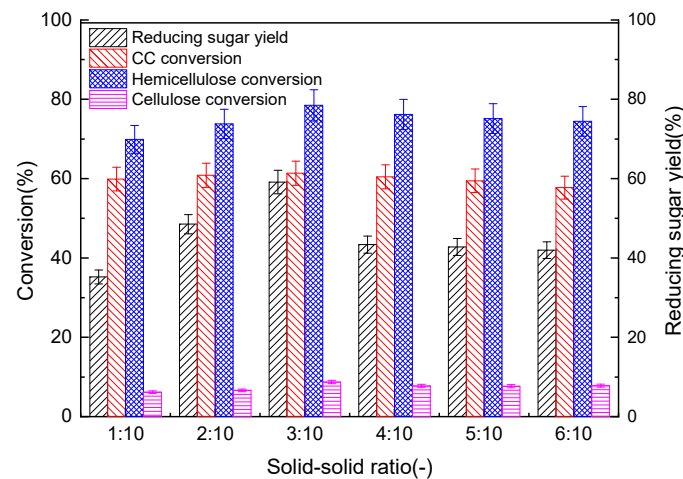


Figure 5. Effects of CW solid-to-solid ratio on the pre-hydro-depolymerization of corn cob (CC particle size of 0.25–0.45 mm, temperature of 160 °C, stirring speed of 600 r/min, time of 2 h, H₂ pressure of 1.5 MPa, CAC solid-to-liquid ratio of 1:10).

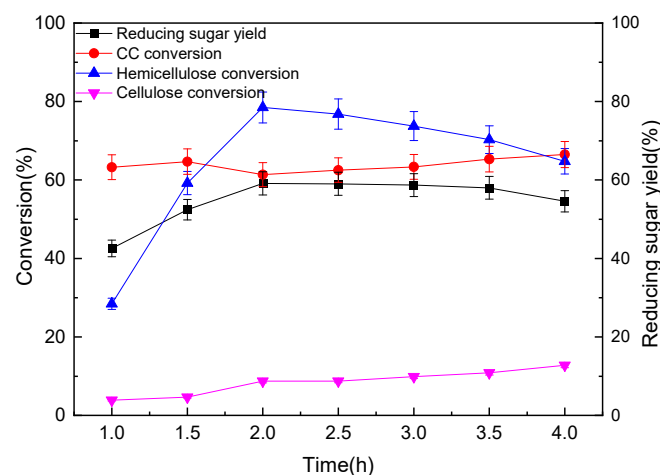


Figure 6. Effects of time on the pre-hydro-depolymerization of corn cob (CC particle size at 0.25–0.45 mm, temperature at 160 °C, stirring speed at 600 r/min, H₂ pressure at 1.5 MPa, CAC solid-to-liquid ratio at 1:10, CW solid-to-solid ratio at 3:10).

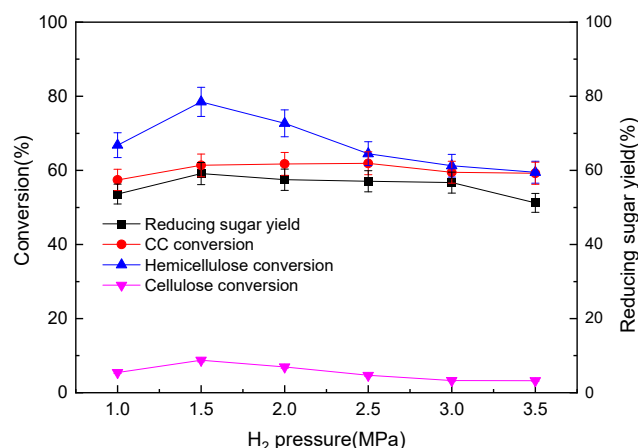


Figure 7. Effects of H₂ pressure on the pre-hydro-depolymerization of corn cob (CC particle size at 0.25–0.45 mm, temperature at 160 °C, stirring speed at 600 r/min, time at 2 h, CAC solid-to-liquid ratio at 1:10, CW solid-to-solid ratio at 3:10).

3.2.1. Effects of Particle Size on the Pre-Hydro-Depolymerization of CC

The impact of the particle size of CC on pre-hydro-depolymerization was examined, and Figure 1 shows that with a gradual reduction in the CC particle size, the hemicellulose conversion rate and RSY increased initially and then decreased, whereas the raw CC conversion rate showed a slow increase. The fixed factors were as follows: the temperature was at 150 °C, time at 2 h, H₂ pressure at 1.5 MPa, CAC solid-to-liquid ratio at 1:10, CW solid-to-solid ratio at 3:10, and stirring speed at 500 r/min. When the CC particle size decreased from >0.90 mm to 0.25–0.45 mm, the hemicellulose conversion rate saw a remarkable increase from 20.95% to 57.48%, alongside this, the RSY increased from 30.37% to 44.23%. At the particle size of 0.25–0.45 mm, the cellulose conversion rate reached its peak at 8.45%. Moreover, the CC conversion rate was observed to be 58.35%. According to Cousins et al. [45], the milling size was found to be correlated to subsequent hydrolysis yields because of an increased surface area-to-volume ratio. With the reduction of the CC particle size, the porosity and surface area of CC increased, promoting better adhesion of the catalyst to the surface of CC and enhancing the catalytic hydrogenation effect. This led to higher conversion rates of hemicellulose, cellulose, and CC and an increased RSY. However, when the particle size was too small, the contact effect with the smaller catalyst particle size was poor, leading to decreased degradation efficiency and poor hydro-degradation outcomes. Therefore, the CC particle size of 0.25–0.45 mm was selected for further analysis.

3.2.2. Influences of Stirring Speed on the Pre-Hydro-Depolymerization of CC

The effect of the stirring speed on the pre-hydro-depolymerization of CC was investigated, and the findings are depicted in Figure 2. Stirring speed mainly affected the hemicellulose conversion rate, whereas it slightly affected the RSY and CC and cellulose conversion rates. The hemicellulose conversion rate gradually increased and reached a maximum of 69.65% at 600 r/min. Hemicellulose conversion rates remained stable when the stirring speed exceeded 600 r/min. Because the reaction was a heterogeneous catalytic reaction, where solid, liquid, and gas states coexist, the mass transfer performance of the reaction directly affected the pre-hydro-degradation of CC. Consequently, the speed of 600 r/min was used in subsequent experiments.

3.2.3. Impacts of Temperature on the Pre-Hydro-Depolymerization of CC

Figure 3 illustrates the significant impact of reaction temperature on the hydro-degradation of CC. With the increasing temperature (120–170 °C), the hemicellulose conversion rate and RSY displayed an initial rapid increase, followed by a subsequent decrease, whereas the CC and cellulose conversion rates exhibited a slow and stable rise. At 120 °C,

the CC conversion rate was only 36.30%, whereas the hemicellulose conversion rate was a mere 3.82%, which was possibly due to the dissolution of soluble substances in CC and the presence of sugars as polysaccharides. By elevating the temperature to 160 °C, the maximum hemicellulose conversion rate (78.74%) and RSY (59.12%) were achieved, while the CC conversion rate reached 61.35%, and the cellulose conversion rate was 8.73%. The reaction temperature was identified as an essential factor affecting the catalytic hydrogenation of CC, which is consistent with Liang et al.'s research, with a glucose yield of 76.8 g/kg and a xylose yield of 118.4 g/kg obtained from the hydrolysis of hemicellulose at 150 °C for 3 h [6]. At low temperatures, the energy of the reaction system was inadequate to attain the activation required to break the C–O bonds between macromolecules, resulting in poor degradation efficiency [40]. In contrast, increasing the reaction temperature increased the kinetic energy of the molecules, enabling them to reach the activation energy threshold, thereby accelerating the hydro-degradation reaction rate and increasing both the hemicellulose conversion rate and RSY. However, excessively high temperatures caused sugars in the CC degradation solution to undergo carbonization and coking, resulting in adhesive deposits on the catalyst surface and reduced catalyst activity. This, along with the subsequent hydrogenation of sugars or the generation of byproducts, ultimately decreased the sugar yield and hemicellulose conversion rate. Conversely, the raw material conversion rate remained unchanged, impeding the subsequent use of sugars. Therefore, a reaction temperature of 160 °C was chosen for subsequent experiments.

3.2.4. Effects of CAC Solid-to-Liquid Ratio on The Pre-Hydro-Depolymerization of CC

The influence of CW solid-to-liquid ratio on the hydro-degradation of CC was investigated (as shown in Figure 4). The conversion efficiency of CC and the degradation rate of cellulose were only slightly affected by the solid-to-liquid ratio, while the conversion rate of hemicellulose and RSY were greatly impacted. As the solid-to-liquid ratio decreased from 1:7 to 1:10, there was a 47.71% and 37.63% increase in the hemicellulose conversion rate and RSY, respectively. The hemicellulose conversion rate and RSY peaked at 78.48% and 59.12%, respectively, whereas a further decrease in the solid-to-liquid ratio resulted in a decrease in CC conversion rate and RSY. Under high-temperature conditions, hot water, the acetyl group of acetic acid in the hemicellulose molecule, and H⁺ played a catalytic role, resulting in a weakly acidic degradation solution [23]. When the solid-to-liquid ratio was high and water content was low, the fluidity of the reaction system and the mass transfer effect were poor, decreasing the available H⁺ ions for the reaction and leading to a low RSY and hemicellulose conversion rate. Conversely, when more water molecules participated in the reaction, active hydrogen molecules increased, promoting the hydro-degradation of hemicellulose. According to our previous study [40], the mechanism of the hydro-depolymerization of rice straw was related to the synergistic effect of in situ acid and metal catalysis. However, hot water had a limited dissolution effect; increasing water volume resulted in CC accumulation and the catalyst settling at the bottom of the reactor, decreasing catalytic performance and resulting in a stable RSY. Thus, the solid-to-liquid ratio of 1:10 was selected for further experiments.

3.2.5. Impacts of CW Solid-to-Solid Ratio on The Pre-Hydro-Depolymerization of CC

Referring to Figure 5, it can be observed that the ratio of CAC solid-to-solid had an obvious impact on RSY and had a slight effect on the conversion of CC, hemicellulose, and cellulose. When the solid-to-solid ratio was from 1:10 to 3:10, the RSY increased from 35.22% to 59.12%, indicating a 24.10% increase. However, when the solid-to-solid ratio exceeded 3:10, the RSY decreased and showed a stable trend. At ratios lower than 3:10, the catalyst amount in the reaction system was insufficient and the CC pre-hydro-degradation solution was not fully utilized. When the catalyst and CC mass ratio was 3:10, the reaction system reached an equilibrium state and the RSY was at its highest. Increasing the solid-to-solid ratio in the presence of the excessive catalyst led to the production of small amounts of other substances, including sugar alcohol, alongside sugars in the CC hydro-degradation

solution. As a result of underutilized excessive catalyst, there was a waste of resources. Therefore, a solid-to-solid ratio of 3:10 was considered for further experiments.

3.2.6. Influences of Time on The Pre-Hydro-Depolymerization of CC

The effect of the reaction time on the hydro-degradation of CC was investigated (as shown in Figure 6). The results showed that the hemicellulose conversion rate and RSY were greatly influenced by the reaction time. Initially, with the extension of the reaction time, the hemicellulose conversion rate and RSY first increased, followed by a decrease, while the CC and cellulose conversion rates increased slowly. The maximum conversion appeared at 2 h. It was found that the main components of monosaccharides in the CC degradation solution were xylose, glucose, and arabinose, among which the xylose content was the highest [6]. The polysaccharides mainly included cellobiose and xylan. At short reaction times, hemicellulose in CC was partially degraded to xylan and other oligosaccharides, resulting in a low monosaccharide content in the hydrolysate, which in turn led to a low hemicellulose conversion rate. As the reaction time was extended, the polysaccharides in the degradation solution were hydro-degraded into monosaccharides, resulting in increased RSY and hemicellulose, and cellulose conversion rates. However, prolonged pre-hydro-depolymerization could lead to increased raw material and cellulose conversion rates but could also result in undesirable degradation of dissolved sugars, which might be converted to sugar alcohols and other byproducts [6]. As a result, the hemicellulose conversion rate and RSY decreased. Ultimately, the optimal reaction time was found to be 2 h.

3.2.7. Influences of H₂ Pressure on the Pre-Hydro-Depolymerization of CC

The effects of hydrogen pressure on CC hydro-degradation were investigated under the following conditions: CC particles, 0.25–0.45 mm; temperature, 160 °C; solid-to-liquid ratio, 1:10; solid-to-solid ratio, 3:10; and stirring speed, 600 r/min. The results, as shown in Figure 7, revealed that the hemicellulose conversion rate was greatly influenced by the hydrogen pressure, increasing initially and then decreasing. Other indexes were minimally affected. The maximum of 78.48% was obtained at a pressure of 1.5 MPa, with CC conversion and RSY, and cellulose conversion rates were 61.35%, 59.12%, and 8.73%, respectively. With the increasing pressure, the molecular weight of hydrogen acting on CC hydro-degradation in the reaction system increased, promoting hemicellulose degradation, which accelerated the reaction and improved the CC conversion rate. However, at high pressure, some monosaccharides in the degradation solution were further catalyzed and hydrogenated into sugar alcohols, leading to a decrease in the monosaccharide content and hemicellulose conversion rate. As high pressure poses safety risks and is not conducive to industrial application, a reaction pressure of 1.5 MPa was selected. These findings can provide useful guidance for optimizing the industrial production of sugars from CC and can contribute to the development of sustainable and eco-friendly biorefineries.

Furthermore, the hydro-depolymerization method described in this study is considered to be a more convenient alternative to the biological approach. This is because hemicellulose is predominantly linked with lignin predominantly through ester covalent bonds due to the presence of hydroxycinnamic acids in lignin-carbohydrate complexes in grasses [46]. Due to its complicated structure, the biological decomposition of hemicellulose requires a set of enzymes, including main-chain-degrading enzymes, to degrade the β -1,4-linked D-xylosidic backbone, and side-chain-degrading enzymes that cleave branched monomers and short oligomers present on the xylan backbone [47].

3.3. Lignin Extraction from Alkali-Treated PHR

To develop a biorefinery-concept-based economy, new feedstock processing strategies and technologies have been developed focusing on the high-quality and high-yield ligno-cellulose component utilization and fractionation of other raw material components for valorized products, such as lignin [15].

3.3.1. Influences of NaOH Concentration on the LER of PHR

The effect of NaOH concentration on the LER was investigated by subjecting PHR to a NaOH concentration gradient of 3~7% under the following conditions: a reaction temperature of 110 °C, a reaction time of 3 h, a solid-to-liquid ratio of 1:10, and stirring speed of 500 r/min. NaOH concentration was found to greatly affect the LER (as shown in Figure 8). The LER initially increased with increasing NaOH concentration and reached a maximum of 70.45% at 6% NaOH, after which it gradually decreased. This is Because low NaOH concentrations were insufficient to effectively break the C–O bond between lignin and cellulose, leading to a low LER. Conversely, high NaOH concentrations led to OH[−] catalyzed bond breaking between lignin and cellulose, as well as promoting the recondensation of exfoliated lignin fragments with residual cellulose. This suggests that excessively high alkali concentrations may induce lignin dissolution, reducing the LER [48]. At a NaOH concentration of 6%, the ester and ether bonds between lignin and cellulose could be completely broken, equilibrating the dissociation and condensation of lignin. This enabled lignin to be dissolved in the solvent to the maximum extent, thereby maximizing the LER. Therefore, an NaOH concentration of 6% was selected for further analysis.

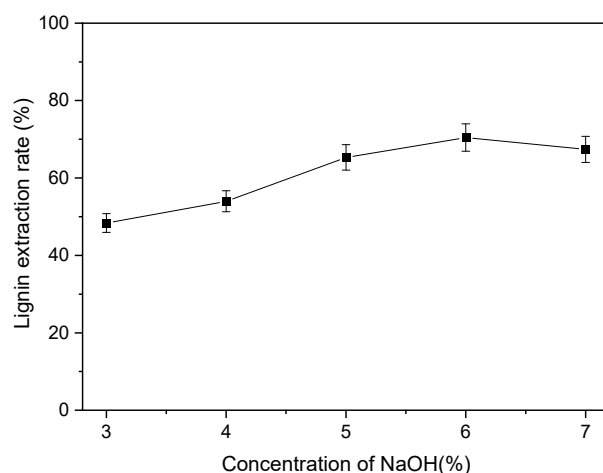


Figure 8. Effects of NaOH concentration on the LER of PHR.

3.3.2. Influences of Temperature on the LER of PHR

The impact of the reaction temperature on the LER was analyzed at temperatures ranging from 80 to 120 °C with a reaction time of 3 h, solid-to-liquid ratio of 1:10, and stirring speed of 500 r/min. The results, displayed in Figure 9, demonstrate that the LER initially increased sharply with the temperature, reaching a maximum of 73.76% at 90 °C, which was 8.78% higher than that observed at 80 °C. Thereafter, the LER slowly decreased to 58.08% at 120 °C. Previous studies have shown that the efficiency of alkali extraction is influenced by the concentration of the solution, reaction duration, and temperature [36,49]. At low temperatures, the C–O bond between lignin and cellulose remained intact, making it difficult to extract lignin. As the temperature increased, the lignin bonds were broken and the production rate of lignin fragments increased. However, at extremely high temperatures, the lignin fragments were broken into small and unrecyclable pieces, reducing the LER. Beyond the temperature of 90 °C, the LER decreased slowly, indicating that higher temperatures were detrimental to the lignin extraction process. Based on these findings, the optimal reaction temperature for achieving a high LER was 90 °C.

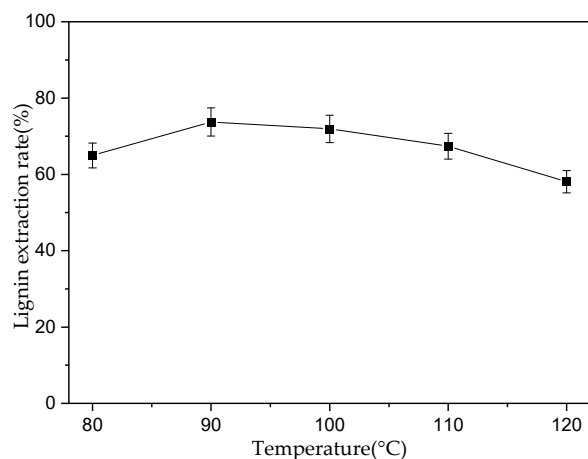


Figure 9. Effects of temperature on the LER of PHR.

3.3.3. Influences of Time on the LER of PHR

The effects of reaction time on the LER were investigated at 6% alkali concentration, a reaction temperature of 90 °C, a solid-to-liquid ratio of 1:10, and a stirring speed of 500 r/min. A graph showing the effect of the reaction time is illustrated in Figure 10. With the reaction time increased, the LER initially increased and then reached a plateau. When the reaction time was 1 h, the LER was 42.78%. However, when the reaction time increased to 3 h, the LER reached 73.76%, which was approximately 1.7 times higher than that at 1 h, and then stabilized, indicating the reaction had reached equilibrium. The results regarding reaction time are consistent with the results of 2% (*w/v*) NaOH treatment at 120 °C, removing 88.59% of CC lignin content [16]. Another study revealed 60~70% lignin recovery using formic acid- and NaOH-pretreated corn stover [39]. The longer the reaction time, the greater the yield of lignin extraction. This was because the longer reaction time allowed for more ester and ether bonds between lignin and cellulose to be broken, making it easier to extract more lignin. However, as the reaction time increased beyond a certain point, the yield of lignin extraction tended to be stable, suggesting that the reaction had reached equilibrium. Therefore, a reaction time of 3 h was chosen for further analysis.

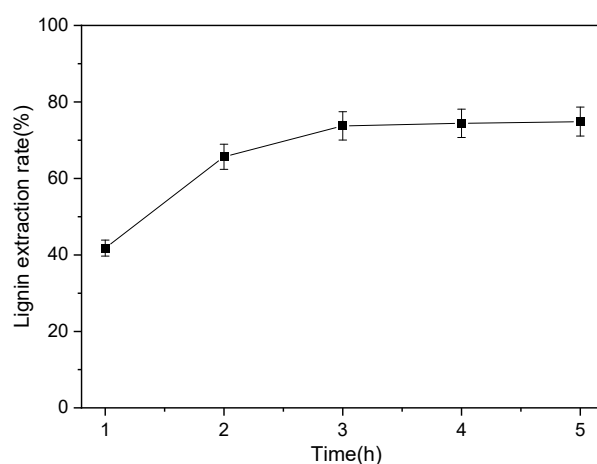


Figure 10. Effects of extraction time on the LER of PHR.

These findings can guide the optimization of lignin extraction processes from PHR and contribute to the development of more effective and sustainable lignin valorization strategies.

3.4. Characterization Results of CC and Hemicellulose- and Lignin-Related Residues

3.4.1. Components and Specific Surface Area of CC and Hemicellulose- and Lignin-Related Residues

The catalytic hydro-depolymerization method was effective in removing hemicellulose molecules from CC, as indicated by a significant decrease in hemicellulose content from $32.5 \pm 1.62\%$ to $2.53 \pm 0.11\%$, resulting in a 96.18% removal of hemicellulose (Table 2). This was consistent with the 91.70% hemicellulose removal in FeCl_3 -pretreated CC as indicated by a previous study [50]. Furthermore, cellulose and lignin contents increased to $53.78 \pm 2.68\%$ and $30.76 \pm 1.53\%$, respectively, with 56.30% cellulose recovery. The removal of hemicellulose did not have a significant effect on the lignin content. After alkali treatment, the remaining hemicellulose components were removed, accompanied by complete lignin dissolution, resulting in a remaining cellulose recovery rate of 46.87%. The specific surface area of CC increased from $2.23 \text{ m}^2/\text{g}$ to $3.50 \text{ m}^2/\text{g}$ after hemicellulose hydro-degradation and further to $4.81 \text{ m}^2/\text{g}$ after lignin removal. Owing to continuous lignin fragmentation after hemicellulose hydro-degradation, cellulose crystallinity decreased, disintegrating the lignocellulosic structure, leading to a loose structure, and thus increasing the specific surface area of CC. However, the CC recovery rates were lower after hemicellulose and lignin removal (38.65% and 22.15%, respectively) compared to acidic pretreatment (49.50%) in a previous study, indicating the severe pre-hydro-depolymerization of CC [51].

Table 2. The changes in component content and surface properties of corn cob and hemicellulose- and lignin-related residues.

Sample	Hemicellulose (%)	Cellulose (%)	Lignin (%)	CC Recovery (%)	Hemicellulose Removal (%)	Cellulose Recovery (%)	Lignin Removal (%)	Specific Surface Area (m^2/g)
CC	32.50 ± 0.62	36.92 ± 1.34	18.22 ± 0.90	-	-	-	-	2.23
PHR	2.53 ± 0.11	53.78 ± 1.68	30.76 ± 1.53	38.65	96.18	56.30	33.06	3.50
PHRD	0	78.13 ± 1.90	0	22.15	100	46.87	100	4.81

CC, corn cob; PHR, pre-hydro-depolymerized CC residues; and PHRD, pre-hydro-depolymerized and delignified CC residues.

3.4.2. FTIR of CC and Hemicellulose- and Lignin-Related Residues

FTIR analyzes the molecular structure and chemical composition, considering differential absorption characteristics of substances at different infrared wavelengths. To determine the effect of hemicellulose and lignin removal, raw CC, PHR, and PHRD were characterized and analyzed by FTIR. The FTIR results are illustrated in Figure 11.

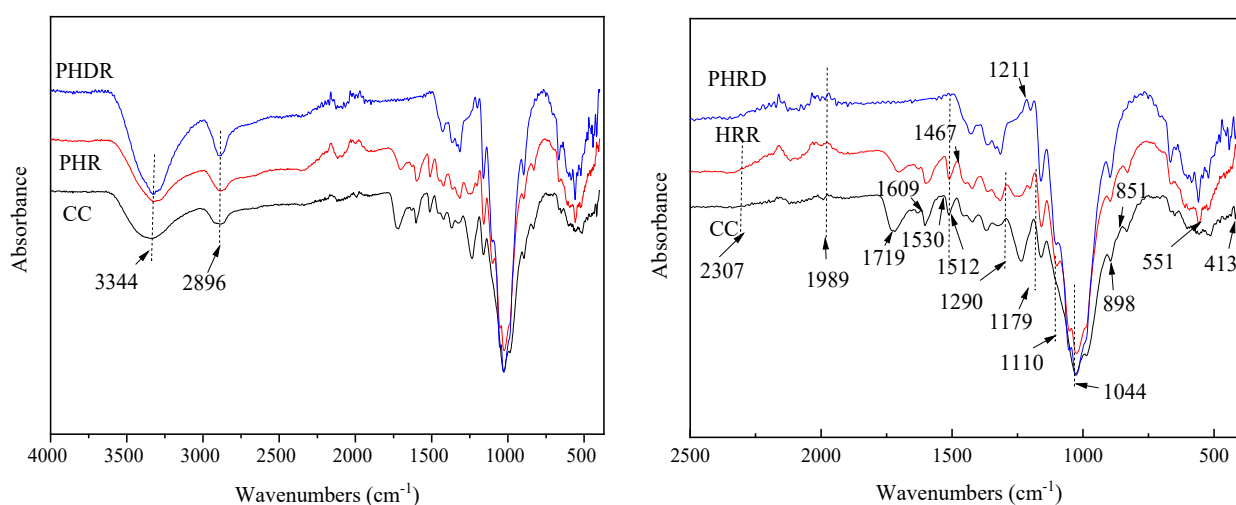


Figure 11. The infrared spectra of corn cob and hemicellulose- and lignin-related residues.

The absorption peak at the wavelengths of $3700\text{--}3300\text{ cm}^{-1}$ belongs to the stretching vibration of the O–H bond, while the peak at $1500\text{--}1300\text{ cm}^{-1}$ corresponds to the bending vibration of the C–H bond (Figure 11). The absorption peak at $1200\text{--}1000\text{ cm}^{-1}$ refers to the stretching vibration of C=C and C–O–C bonds [10]. Comparing CC with PHR, the peak at $1290\text{--}1179\text{ cm}^{-1}$, which was the characteristic peak of the acetyl group, disappeared in xylan, indicating the complete hydro-depolymerization of hemicellulose in CC [52]. In PHRD, the C–H vibrational absorption peak on the para-substituted aromatic ring at 851 cm^{-1} disappeared, whereas the absorption band at 1162 cm^{-1} of C–O–C stretching in cellulose and the peak of the β -1,4 glycosidic bond at 898 cm^{-1} both increased considerably, indicating the removal of hemicellulose and lignin [40,53,54]. The vibrational absorption peaks of the aromatic ring skeleton at $1609\text{--}1512\text{ cm}^{-1}$ disappeared [54,55], and the C=O stretching vibration peaks in nonconjugated carbonyl, carboxyl, and ester groups at 1719 cm^{-1} also disappeared [40], demonstrating the removal of lignin in CC. After the removal of hemicellulose and lignin, the absorption peak at $2317\text{--}1968\text{ cm}^{-1}$ changed, indicating severe damage to molecular structures. The characteristic peak of cellulose at $1102\text{--}1044\text{ cm}^{-1}$ weakened, revealing the partial degradation of cellulose [56,57]. A strong absorption peak at approximately 3344 cm^{-1} represented the overlapping peak of –OH in cellulose as reported by Sun et al. [58]. Meanwhile, Louis et al. attributed the absorbance band at 2896 cm^{-1} to the C–H or CH_2 stretching vibration [52]. Following hemicellulose removal, the peak at 2896 cm^{-1} underwent a change, suggesting that the microcrystalline structure of cellulose remains unharmed. On the other hand, lignin removal resulted in a significant change in the peak at 2896 cm^{-1} , implying a reduced crystallinity and polymerization degree of cellulose. Additionally, the absorption peak in the $1000\text{--}400\text{ cm}^{-1}$ fingerprint region underwent considerable changes, pointing to a shift in the molecular structure of CC during pre-hydro-degradation.

3.4.3. SEM of CC and Hemicellulose- and Lignin-Related Residues

To evaluate the surface morphology and microstructural changes of CC and its residues after hemicellulose and lignin removal, SEM characterization was performed, and the results are presented in Figure 12A–C.

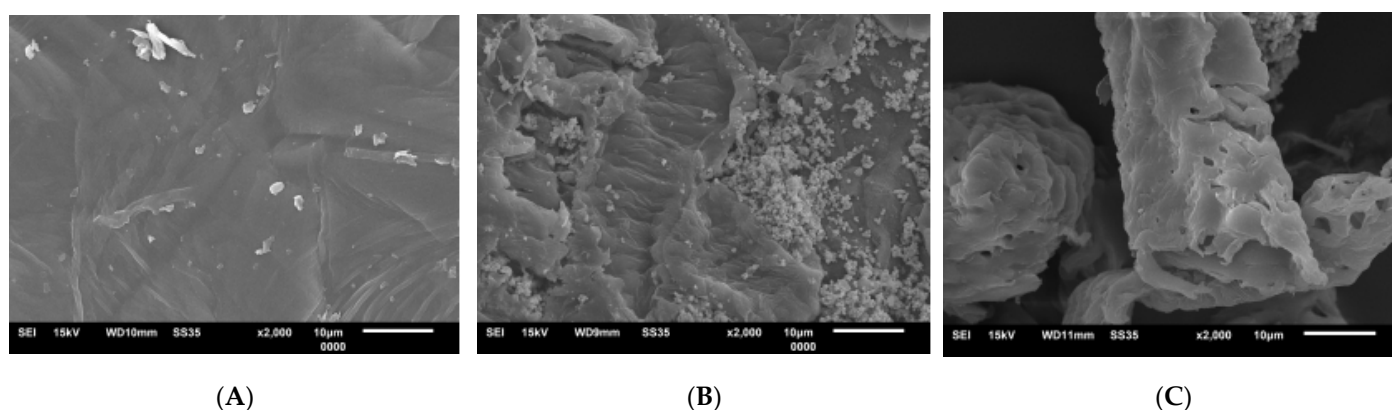


Figure 12. The scanning electron microscope spectrum of CC and hemicellulose- and lignin-related residues. (A) CC; (B) residues after hemicellulose removal; and (C) hemicellulose removal delignification.

Raw CC showed a dense surface with flat and smooth fiber bundles, which are tightly arranged without gaps or broken marks (Figure 12A) [59,60]. Upon hemicellulose removal, the surface became loose and uneven with broken residues, and the flat surface disappeared, revealing a damaged CC surface structure (Figure 12B) [56]. After continuous lignin removal, the residues were characterized by an increase in pore density and size, leading to damage in the 3D structure of CC (Figure 12C). According to Yang et al. and

Louis et al., these changes were a result of xylan release and lignin removal by pre-hydro-depolymerization and delignification [43,52]. The presence of these pores, cracks, and coarsened surfaces could facilitate the adsorption of the hydro-catalyst and the remaining cellulose in CC [56]. The hydro-catalyst is most likely to get absorbed in the pores, subsequently degrading cellulose. Therefore, the pretreatment of hemicellulose and lignin is crucial for the complete utilization of cellulose in subsequent CC.

3.5. Optimization of Cellulose Hydro-Depolymerization in CC

The structure of cellulose is complex as it is encapsulated in a cross-linked hemicellulose/pectin matrix via hydrogen bonds and van der Waals forces, making it difficult to degrade and depolymerize [46]. However, after the release of xylan and the removal of lignin in CC, cellulose becomes more accessible and can be hydro-depolymerized again. To understand the effects of different factors on cellulose and the hydro-degradation of PHRD, a four-factor three-level orthogonal experiment L9 (3^4) was designed based on cellulose conversion and CC conversion rates [61]. The experiment aimed to determine the optimal combination of factors that would maximize the conversion rates for both cellulose and CC. The results of the orthogonal experiment and the processed data are presented in Table 3.

Table 3. Factors and levels of the orthogonal design L9 (3^4) and experimental results for two stability indicators.

Number	Factors				Results	
	A Temperature (°C)	B Solid-Liquid Ratio	C Time (h)	D Solid-Solid Ratio	Cellulose Conversion (%)	CC Conversion (%)
1	1 (140)	1 (1:8)	1 (1)	1 (2:10)	13.57	17.39
2	1 (140)	2 (1:9)	2 (2)	2 (3:10)	36.63	40.42
3	1 (140)	3 (1:10)	3 (3)	3 (4:10)	27.39	44.23
4	2 (150)	1 (1:8)	2 (2)	3 (4:10)	11.92	29.00
5	2 (150)	2 (1:9)	3 (3)	1 (2:10)	18.53	47.06
6	2 (150)	3 (1:10)	1 (1)	2 (3:10)	9.84	21.03
7	3 (160)	1 (1:8)	3 (3)	2 (3:10)	15.37	43.53
8	3 (160)	2 (1:9)	1 (1)	3 (4:10)	20.75	51.16
9	3 (160)	3 (1:10)	2 (2)	1 (2:10)	18.74	47.55
Cellulose conversion		k_1	25.86	13.62	14.72	16.95
		k_2	13.43	25.30	22.43	20.61
		k_3	18.29	18.66	20.43	20.02
		Range R	12.43	11.68	7.71	3.66
		Primary and secondary order	A > B > C > D			
CC conversion		k_1	34.01	29.97	29.86	37.33
		k_2	32.36	46.21	38.99	34.99
		k_3	47.41	37.60	41.46	41.46
		Range R	15.05	16.24	11.60	6.47
		Primary and secondary order	A > B > C > D			
	Optimal horizontal combination	A ₁ B ₂ C ₂ D ₂				
	Optimal horizontal combination	A ₃ B ₂ C ₃ D ₃				

k_1 , k_2 , and k_3 represent the average of the indicators at each level of each factor. k_x is the comprehensive average of level x data = sum of level x of the values/repetition times of level x. Range R is the range of the row, which indicates the extent of the factor's impact on the results. It is calculated as the maximum k value minus the minimum k value.

The optimization conditions for the conversion of cellulose and CC were determined based on the primary and secondary orders of the factors affecting the two indexes. The optimal conditions for cellulose conversion and CC conversion were not the same. The main factor affecting both cellulose and CC conversion was the temperature (factor A). At A₁, cellulose conversion was higher, whereas, at A₃, CC conversion was higher. This was mainly because monosaccharides in the degradation solution were converted into alcohols and other substances at a higher temperature, reducing their contents and the cellulose

conversion rate; therefore, A₁ was selected as factor A. Similarly, B factors (solid-to-liquid ratio) had the same order of effect on indicators, with the highest conversion rates observed at B₂. Factors C (time) and D (solid-to-solid ratio) had the same order of effect on indicators but not the same level. C₂ and D₂ were selected for cellulose conversion, whereas C₃ and D₃ were selected for CC conversion. Therefore, the optimal combination was determined to be A₁B₂C₂D₂ (temperature, 140 °C; solid-to-liquid ratio, 1:9; time, 2 h; and solid-to-solid ratio, 3:10), which resulted in a cellulose conversion rate of 36.63% and a CC conversion rate of 40.42%. These conditions allowed for a four-fold increase in the cellulose conversion rate compared to pre-hydro-depolymerization conditions, while also using a lower temperature. This indicates that cellulose hydro-depolymerization benefits hemicellulose sugar release and lignin removal. The increase observed was consistent with the results of a previous study [21]. Additionally, the sugar yield obtained after tetrabutyl phosphate hydroxide ionic liquid pretreatment and CC enzymatic hydrolysis was also four-fold higher than that obtained from untreated raw materials.

3.6. Multiple Hydro-Depolymerizations of PHRD Residues

Table 4 shows the results of multiple hydro-depolymerization reactions performed on PHRD residues, which exhibited continuous production of sugars and a cumulative cellulose conversion rate of 76.97%, with a CC conversion rate reaching 85.70%. The residues could undergo five successive rounds of hydro-depolymerization, resulting in a gradual decrease in cellulose and CC conversion rates. However, the residues remained capable of producing sugars, indicating that they could still be efficiently hydro-degraded. This is likely due to the continual destruction of the whisker-like structure on the residue surface caused by repeated actions such as filtration, washing, and extrusion during multiple reactions. Although the cellulose conversion in our study was lower than Xu et al.'s [50], where the enzymatic digestibility of pretreated corncob residue was 90.0% after 48 h, the reaction was still highly efficient. These findings provide valuable insights for subsequent industrial applications.

Table 4. The results of multiple hydro-depolymerization reactions performed on PHRD residues.

Reaction Times	1	2	3	4	5
CC conversion (%)	40.42	18.95	12.72	8.37	5.24
Cellulose conversion (%)	36.63	16.89	10.27	8.30	4.88

4. Conclusions

The proposed three-step process enables the coproduction of hemicellulose-derived saccharides, cellulose by hydro-depolymerization, and lignin by alkali pretreatment. Many saccharides were harvested from the hydro-pre-treated hemicellulose, resulting in a hemicellulose conversion rate of $78.48 \pm 3.92\%$, accompanied by a CC conversion rate of 61.35%, and a reducing sugar yield of $59.12 \pm 2.95\%$. The maximum lignin extraction efficiency was $73.76 \pm 3.68\%$, and the optimum cellulose conversion rate was 36.63%, which increased to 76.96% after five cycles of hydro-depolymerization. The integrated process offers a feasible solution for the utilization of CC waste, leading to high-value products. This is not only to reduce waste but also for the development of a circular economy.

Supplementary Materials: The following supporting information can be downloaded at: <https://www.mdpi.com/article/10.3390/su15119041/s1>.

Author Contributions: Conceptualization and writing—original draft, X.Y.; investigation, X.L.; data curation, L.Z.; writing—review and editing, J.L.; writing—review and editing and funding acquisition, J.Z. All authors have read and agreed to the published version of the manuscript.

Funding: This research received no external funding.

Institutional Review Board Statement: Not applicable.

Informed Consent Statement: Not applicable.

Data Availability Statement: The authors declare that they have no known competing financial interests or personal relationships that could have appeared to influence the work reported in this paper.

Conflicts of Interest: The authors declare no conflict of interest.

References

1. Weng, Y.; Wang, Y.; Zhang, M.; Wang, X.; Sun, Q.; Mu, S.; Wang, H.; Fan, M.; Zhang, Y. Selectively chemo-catalytic hydrogenolysis of cellulose to EG and EtOH over porous SiO₂ supported tungsten catalysts. *Catal. Today* **2023**, *407*, 89–95.
2. Chen, M.; Wang, Y.; Lu, J.; Du, J.; Tao, Y.; Cheng, Y.; Li, Q.; Wang, H. Combinatorial pretreatments of reed straw using liquid hot water and lactic acid for fermentable sugar production. *Fuel* **2023**, *331*, 125916.
3. Zheng, H.; Wang, Y.; Feng, X.; Li, S.; Leong, Y.K.; Chang, J.S. Renewable biohydrogen production from straw biomass—Recent advances in pretreatment/hydrolysis technologies and future development. *Int. J. Hydrog. Energ.* **2022**, *47*, 37359–37373.
4. Zahoor; Wang, W.; Tan, X.; Imtiaz, M.; Wang, Q.; Miao, C.; Yuan, Z.; Zhuang, X. Rice straw pretreatment with KOH/urea for enhancing sugar yield and ethanol production at low temperature. *Ind. Crop. Prod.* **2021**, *170*, 113776.
5. Zhao, J.; Tao, X.; Li, J.; Jia, Y.; Shao, T. Enhancement of biomass conservation and enzymatic hydrolysis of rice straw by dilute acid-assisted ensiling pretreatment. *Bioresour. Technol.* **2021**, *320*, 124341. [PubMed]
6. Liang, J.; Li, Z.; Dai, S.; Tian, G.; Wang, Z. Production of hemicelluloses sugars, cellulose pulp, and lignosulfonate surfactant using corn stalk by prehydrolysis and alkaline sulfite cooking. *Ind. Crop. Prod.* **2023**, *192*, 115880.
7. He, S.; Wang, J.; Cheng, Z.; Dong, H.; Yan, B.; Chen, G. Synergetic effect and primary reaction network of corn cob and cattle manure in single and mixed hydrothermal liquefaction. *J. Anal. Appl. Pyrol.* **2021**, *155*, 105076.
8. Mihajlovski, K.; Pecarski, D.; Rajilić-Stojanović, M.; Dimitrijević-Branković, S. Valorization of corn stover and molasses for enzyme synthesis, lignocellulosic hydrolysis and bioethanol production by *Hymenobacter* sp. CKS3. *Environ. Technol. Inno.* **2021**, *23*, 101627.
9. Maleki, M.; Ariaeenejad, S.; Salekdeh, G.H. Efficient saccharification of ionic liquid- pretreated rice straw in a one-pot system using novel metagenomics derived cellulases. *Bioresour. Technol.* **2022**, *345*, 126536.
10. Laltha, M.; Sewsynker-Sukai, Y.; Gueguim Kana, E.B. Development of microwave-assisted alkaline pretreatment methods for enhanced sugar recovery from bamboo and corn cobs: Process optimization, chemical recyclability and kinetics of bioethanol production. *Ind. Crop. Prod.* **2021**, *174*, 114166.
11. Qiao, H.; Han, M.; Ouyang, S.; Zheng, Z.; Ouyang, J. An integrated lignocellulose biorefinery process: Two-step, sequential treatment with formic acid for efficiently producing ethanol and furfural from corn cobs. *Renew. Energ.* **2022**, *191*, 775–784.
12. Norazlina, I.; Dhinashini, R.S.; Nurhafizah, I.; Norakma, M.N.; Noor Fazreen, D. Extraction of xylose from rice straw and lemongrass via microwave assisted. *Mater. Today Proc.* **2022**, *48*, 784–789.
13. Liu, C.; Wang, C.; Yao, H.; Chapman, S.J. Pretreatment is an important method for increasing the conversion efficiency of rice straw by black soldier fly larvae based on the function of gut microorganisms. *Sci. Total Environ.* **2021**, *762*, 144118. [PubMed]
14. Woo, W.; Tan, J.; Tan, J.; Indera Luthfi, A.; Abdul, P.; Abdul Manaf, S.; Yeap, S.K. An insight into enzymatic immobilization techniques on the saccharification of lignocellulosic biomass. *Ind. Eng. Chem. Res.* **2022**, *61*, 10603–10615.
15. Lin, Q.; Yan, Y.; Liu, X.; He, B.; Wang, X.; Wang, X.; Liu, C.; Ren, J. Production of xylooligo-saccharide, nanolignin, and nanocellulose through a fractionation strategy of corncob for biomass valorization. *Ind. Eng. Chem. Res.* **2020**, *59*, 17429–17439.
16. Ratna, A.S.; Ghosh, A.; Mukhopadhyay, S. Advances and prospects of corn husk as a sustainable material in composites and other technical applications. *J. Clean. Prod.* **2022**, *371*, 133563.
17. Zhang, H.; Wu, J. Statistical optimization of aqueous ammonia pretreatment and enzymatic hydrolysis of corn cob powder for enhancing sugars production. *Biochem. Eng. J.* **2021**, *174*, 108106.
18. Lee, K.T.; Chen, W.H.; Sarle, P.; Park, Y.K.; Ok, Y.S. Recover energy and materials from agricultural waste via thermochemical conversion. *Earth* **2022**, *11*, 1200–1204.
19. Zhang, Y.; Guo, S.; Wang, Y.; Liang, X.; Xu, P.; Gao, C.; Ma, C. Production of d-xylonate from corn cob hydrolysate by a metabolically engineered *Escherichia coli* strain. *ACS Sustain. Chem. Eng.* **2019**, *7*, 2160–2168.
20. Ling, R.; Wei, W.; Jin, Y. Pretreatment of sugarcane bagasse with acid catalyzed ethylene glycol-water to improve the cellulose enzymatic conversion. *Bioresour. Technol.* **2022**, *361*, 127723.
21. Sun, J.; Ding, R.; Yin, J. Pretreatment of corn cobs and corn stalks with tetrabutyl phosphate hydroxide ionic liquid to enhance enzymatic hydrolysis process. *Biochem. Eng. J.* **2022**, *177*, 108270.
22. Kucharska, K.; Rybarczyk, P.; Hołowacz, I.; Konopacka-Lyskawa, D.; Słupek, E.; Makoś, P.; Cieśliński, H.; Kamiński, M. Influence of alkaline and oxidative pre-treatment of waste corn cobs on biohydrogen generation efficiency via dark fermentation. *Biomass Bioenergy* **2020**, *141*, 105691.
23. Martins-Vieira, J.C.; Lachos-Perez, D.; Draszewski, C.P.; Celante, D.; Castilhos, F. Sugar, hydrochar and bio-oil production by sequential hydrothermal processing of corn cob. *J. Supercrit. Fluid.* **2023**, *194*, 105838.

24. de Mello Captti, C.C.; Pellegrini, V.O.A.; Espirito Santo, M.C.; Cortez, A.A.; Falvo, M.; de Curvelo, A.A.S.; Campos, E.; Filgueiras, J.G.; Guimaraes, F.E.G.; de Azevedo, E.R.; et al. Enzymatic production of xylooligosaccharides from corn cobs: Assessment of two different pretreatment strategies. *Carbohydr. Polym.* **2023**, *299*, 12074.
25. Wang, W.; Cao, X.; Guo, H.; Yang, X.; Guo, N.; Ma, Y. Carbon-based solid acid derived from lignin and polyvinyl chloride for conversion of xylose and crop wastes to furfural. *Mol. Catal.* **2022**, *524*, 112329.
26. Long, Y.; Ma, Y.; Wan, J.; Wang, Y.; Tang, M.; Zheng, Q.; Ma, Y. Hydrolysate from the enzymatic treatment of corn cob as a carbon source for heterotrophic denitrification process. *Water Process Eng.* **2023**, *51*, 103473.
27. Sun, J.; Ding, R.; Yin, J. Pretreatment corn ingredient biomass with high pressure CO₂ for conversion to fermentable sugars via enzymatic hydrolysis of cellulose. *Ind. Crop. Prod.* **2022**, *177*, 114518.
28. Tsegaye, B.; Balomajumder, C.; Roy, P. Organosolv pretreatment of rice straw followed by microbial hydrolysis for efficient biofuel production. *Renew. Energy.* **2020**, *148*, 923–934.
29. Hussin, M.H.; Rahim, A.A.; Mohamad, I.M.N.; Yemloul, M.; Perrin, D.; Brosse, N. Investigation on the structure and antioxidant properties of modified lignin obtained by different combinative processes of oil palm fronds (OPF) biomass. *Ind. Crop. Prod.* **2014**, *52*, 544–551.
30. Sartika, D.; Firmansyah, A.P.; Junais, I.; Arnata, I.W.; Fahma, F.; Firmanda, A. High yield production of nanocrystalline cellulose from corn cob through a chemical-mechanical treatment under mild conditions. *Int. J. Biol. Macromol.* **2023**, *240*, 124327.
31. Islam, M.T.; Sultana, A.I.; Saha, N.; Klinger, J.L.; Reza, M.T. Pretreatment of biomass by selected type-III deep eutectic solvents and evaluation of the pretreatment effects on hydrothermal carbonization. *Ind. Eng. Chem. Res.* **2021**, *60*, 15479–15491.
32. Chiranjeevi, T.; Mattam, A.J.; Vishwakarma, K.K.; Uma, A.; Peddy, V.C.R.; Gandham, S.; Velankar, H.R. Assisted single-step acid pretreatment (ASAP) process for enhanced delignification of rice straw for bioethanol production. *ACS Sustain. Chem. Eng.* **2018**, *6*, 8762–8774.
33. Zhong, L.; Wang, C.; Xu, M.; Ji, X.; Yang, G.; Chen, J.; Janaswamy, S.; Lyu, G. Alkali-catalyzed organosolv pretreatment of lignocellulose enhances enzymatic hydrolysis and results in highly antioxidative lignin. *Energy. Fuel.* **2021**, *35*, 5039–5048.
34. Aghaei, S.; Karimi Alavijeh, M.; Shafiei, M.; Karimi, K. A comprehensive review on bioethanol production from corn stover: Worldwide potential, environmental importance, and perspectives. *Biomass Bioenergy.* **2022**, *161*, 106447.
35. Aggarwal, N.; Pal, P.; Sharma, N.; Saravanamurugan, S. Consecutive organosolv and alkaline pretreatment: An efficient approach toward the production of cellulose from rice straw. *ACS Omega* **2021**, *6*, 27247–27258.
36. Lima, C.S.; Rabelo, S.C.; Ciesielski, P.N.; Roberto, I.C.; Rocha, G.J.M.; Driemeier, C. Multiscale alterations in sugar cane bagasse and straw submitted to alkaline deacetylation. *ACS Sustain. Chem. Eng.* **2018**, *6*, 3796–3804.
37. Khan, M.F.S.; Akbar, M.; Xu, Z.; Wang, H. A review on the role of pretreatment technologies in the hydrolysis of lignocellulosic biomass of corn stover. *Biomass Bioenergy.* **2021**, *155*, 106276.
38. Abdolmaleki, A.; Nabavizadeh, S.S.; Badbedast, M. 1-(Carboxymethyl)pyridinium chloride as an acidic ionic liquid for rice straw effective pretreatment. *Renew. Energy.* **2021**, *177*, 544–553.
39. Saulnier, B.K.; Siahkamari, M.; Singh, S.K.; Nejad, M.; Hodge, D.B. Effect of dilute acid pretreatment and lignin extraction conditions on lignin properties and suitability as a phenol replacement in phenol-formaldehyde wood adhesives. *J. Agric. Food Chem.* **2023**, *71*, 592–602.
40. Yang, X.; Zhao, J.; Liang, J.; Zhu, J. Efficient and selective catalytic conversion of hemicellulose in rice straw by metal catalyst under mild conditions. *Sustainability* **2020**, *12*, 106011.
41. Sluiter, A.; Hames, B.; Ruiz, R.; Scarlata, C.; Templeton, D. Determination of structural carbohydrates and lignin in biomass. *Lab. Anal. Proced.* **2008**, *1671*, 1–15.
42. Miller, G.L. Use of dinitrosalicylic acid reagent for determination of reducing sugar. *Anal. Chem.* **1959**, *31*, 426–428.
43. Yang, M.; Gao, X.; Lan, M.; Dou, Y.; Zhang, X. Rapid fractionation of lignocellulosic biomass by p-TsOH pretreatment. *Energy. Fuel* **2019**, *33*, 2258–2264.
44. Han, Y.; Xu, J.; Zhao, Z.; Zhao, J. Analysis of enzymolysis process kinetics and estimation of the resource conversion efficiency to corn cobs with alkali soaking, water and acid steam explosion pretreatments. *Bioresour. Technol.* **2018**, *264*, 391–394. [[PubMed](#)]
45. Cousins, D.S.; Pedersen, K.P.; Otto, W.G.; Rony, A.H.; Lacey, J.A.; Aston, J.E.; Hodge, D.B. Particle classification by image analysis improves understanding of corn stover degradation mechanisms during deconstruction. *Ind. Crop. Prod.* **2023**, *193*, 116153.
46. Tocco, D.; Carucci, C.; Monduzzi, M.; Salis, A.; Sanjust, E. Recent developments in the delignification and exploitation of grass lignocellulosic biomass. *ACS Sustain. Chem. Eng.* **2021**, *9*, 2412–2432.
47. Zhang, R.; Lin, D.; Zhang, L.; Zhan, R.; Wang, S.; Wang, K. Molecular and biochemical analyses of a novel trifunctional endoxylanase/endoglucanase/feruloyl esterase from the human colonic bacterium *Bacteroides intestinalis* DSM 17393. *J. Agric. Food Chem.* **2022**, *70*, 4044–4056.
48. Wang, Y.; Gong, X.; Hu, X.; Zhou, N. Lignin monomer in steam explosion assist chemical treated cotton stalk affects sugar release. *Bioresour. Technol.* **2019**, *276*, 343–348.
49. Cai, D.; Li, P.; Luo, Z.; Qin, P.; Chen, C.; Wang, Y.; Wang, Z.; Tan, T. Effect of dilute alkaline pretreatment on the conversion of different parts of corn stalk to fermentable sugars and its application in acetone–butanol–ethanol fermentation. *Bioresour. Technol.* **2016**, *211*, 117–124.
50. Xu, Q.; Yang, W.; Liu, G.; Liang, C.; Lu, S.; Qi, Z.; Hu, J.; Wang, Q.; Qi, W. Enhanced enzymatic hydrolysis of corncob by synthesized enzyme-mimetic magnetic solid acid pretreatment in an aqueous phase. *ACS Omega* **2019**, *4*, 17864–17873.

51. Li, P.; Cai, D.; Luo, Z.; Qin, P.; Chen, C.; Wang, Y.; Zhang, C.; Wang, Z.; Tan, T. Effect of acid pretreatment on different parts of corn stalk for second generation ethanol production. *Bioresour. Technol.* **2016**, *206*, 86–92.
52. Louis, A.C.F.; Venkatachalam, S. Energy efficient process for valorization of corn cob as a source for nanocrystalline cellulose and hemicellulose production. *Int. J. Biol. Macromol.* **2020**, *163*, 260–269.
53. Sharma, K.; Khaire, K.C.; Thakur, A.; Moholkar, V.S.; Goyal, A. Acacia xylan as a substitute for commercially available xylan and its application in the production of xylooligosaccharides. *ACS Omega* **2020**, *5*, 13729–13738.
54. Yang, X.; Li, X.; Liang, J.; Zhu, J. Comparative study of effective pretreatments on the structural disruption and hydrodepolymerization of rice straw. *Sustainability* **2023**, *15*, 4728.
55. Jackson, M.A.; Price, N.P.J.; Blackburn, J.A.; Peterson, S.C.; Kenar, J.A.; Haasch, R.T.; Chen, C. Partial hydrodeoxygenation of corn cob hydrolysate over palladium catalysts to produce 1-hydroxy-2-pentanone. *Appl. Catal. A-Gen.* **2019**, *577*, 52–61.
56. Hu, H.; Liang, W.; Zhang, Y.; Wu, S.; Yang, Q.; Wang, Y.; Zhang, M.; Liu, Q. Multipurpose use of a corncob biomass for the production of polysaccharides and the fabrication of a biosorbent. *ACS Sustain. Chem. Eng.* **2018**, *6*, 3830–3839.
57. Guo, X.Y.; Zhang, T.; Shu, S.T.; Zheng, W.; Gao, M.T. Compositional and Structural Changes of Corn cob pretreated by electron beam irradiation. *ACS Sustain. Chem. Eng.* **2016**, *5*, 420–425.
58. Sun, Y.; Xu, J.; Xu, F.; Su, R. Efficient separation and physico-chemical characterization of lignin from eucalyptus using ionic liquid-organic solvent and alkaline ethanol solvent. *Ind. Crop. Prod.* **2013**, *47*, 277–285.
59. Zou, H.; Jiang, Q.; Zhu, R.; Chen, Y.; Sun, T.; Li, M.X.; Zhai, J.; Shi, D.; Ai, H.; Gu, L.; et al. Enhanced hydrolysis of lignocellulose in corn cob by using food waste pretreatment to improve anaerobic digestion performance. *J. Environ. Manag.* **2020**, *254*, 109830.
60. Guo, X.; Shu, S.; Zhang, W.; Wang, E.; Hao, J. Synergetic degradation of corn cob with inorganic salt (or hydrogen peroxide) and electron beam irradiation. *ACS Sustain. Chem. Eng.* **2016**, *4*, 1099–1105.
61. Liao, M.H.; Jin, R.T.; Ren, H.W.; Shang, J.Q.; Kang, J.X.; Xin, Q.Y.; Liu, N.; Li, M. Orthogonal experimental design for the optimization of four additives in a model liquid infant formula to improve its thermal stability. *LWT—Food Sci. Technol.* **2022**, *163*, 113495.

Disclaimer/Publisher’s Note: The statements, opinions and data contained in all publications are solely those of the individual author(s) and contributor(s) and not of MDPI and/or the editor(s). MDPI and/or the editor(s) disclaim responsibility for any injury to people or property resulting from any ideas, methods, instructions or products referred to in the content.